

**EFFECTS OF EPIMUSCULAR MYOFASCIAL FORCE
TRANSMISSION ON SENSORY LEVEL: EXPERIMENTAL
ASSESSMENT BY AFFERENT SIGNALS RECEIVED
FROM FROG LOWER LEG MUSCLES**

by

Önder Emre Arıkan

B.Sc., Molecular Biology and Genetics, Istanbul Technical University, 2006

Submitted to the Institute of Biomedical Engineering

in partial fulfillment of the requirements

for the degree of

Master of Science

in

Biomedical Engineering

Boğaziçi University

2009

**EFFECTS OF EPIMUSCULAR MYOFASCIAL FORCE
TRANSMISSION ON SENSORY LEVEL: EXPERIMENTAL
ASSESSMENT BY AFFERENT SIGNALS RECEIVED
FROM FROG LOWER LEG MUSCLES**

APPROVED BY:

Assist. Prof. Dr. Can A. Yücesoy
(Thesis Advisor)

Assist. Prof. Dr. Burak Güçlü

Prof. Dr. Hale Saybaşıli

DATE OF APPROVAL: 28 August 2009

ACKNOWLEDGMENTS

First and foremost I'd like to thank my supervisor Can A. Yücesoy. His support, endless patience and insistence on treating his students as a colleague rather than an underling made me feel privileged all the time. His teachings serve far beyond academia and I owe him a lot.

Assist. Prof. Burak Güçlü never hesitated in taking the time to share his expertise and advices and certainly big portion of this work is because of him.

Prof. Dr. Hale Saybaşılı provided valuable comments during my committee meetings and helped me see several keypoints that would still be missing if not for her.

Filiz Ateş has been the best friend and a reliable mentor since the first day I joined the Biomechanics Lab. I can't thank her enough.

Sevinç Mutlu took me as an apprentice and tried to teach all she knew about electrophysiology. She is also a very good friend who deserves her name.

Daniel A. Press is the best lab mate, who is always very insightful about pretty much everything. I was really lucky that he was nearby during the final stages of my work.

Özgür Tabakoğlu and Nermin Topaloğlu of the Biophotonics Lab has always been welcoming even at times when I constantly nagged them for microscopy and other stuff.

Mehmet Kocatürk was a really good friend and he showed me really nice coding tricks which helped me build my own code. I thank him for all.

Deniz Nevşehirli and Murat Tümer of Instrumentation Lab were really handy guys. They helped me with solutions for my experimental set-up and other issues like getting things done in 'the Institute'.

Çiğdem Günsür Çelik and Aynur Abla of the secretary were always welcoming in helping with administrative issues. Their patience will be remembered.

Yusuf Abi, Derviş Abi, Erhan Abi and İbrahim Usta were really helpful in resolving some seemingly minor problems which could have turned major if they hadn't helped.

Last but definitely not the least I want to thank Arıkan family (my mom Gülşen, my dad Necmi and my brother Eren) for their tremendous support to young scientist candidates. Not only they funded the work entirely but also helped when sometimes motivation was bit of an issue.

ABSTRACT

EFFECTS OF EPIMUSCULAR MYOFASCIAL FORCE TRANSMISSION ON SENSORY LEVEL: EXPERIMENTAL ASSESSMENT BY AFFERENT SIGNALS RECEIVED FROM FROG LOWER LEG MUSCLES

It has been shown that non-tendinous structures play a major role in force transmission: epimuscular myofascial force transmission. Such force transmission was shown to cause substantial strain distributions along muscle fibers indicating serial heterogeneity of sarcomere lengths. Recent studies showed evidence on sizable inter-antagonistic epimuscular myofascial force transmission. It is hypothesized in this study that epimuscular myofascial force transmission can play a role in afferent signals generated in muscle sensory organs. The goal of our present study was to test this hypothesis by measuring the afferent firing rates of antagonistic muscles of the lower leg. Gastrocnemius muscle of the frog (*Rana ridibunda*) was given 1-5 mm of ramp-and-hold stretch via a pulley mechanism connected to its distal tendon. Keeping the ankle and knee angles fixed (at 100° and 120°, respectively), sensory unit recordings were taken from both tibial and peroneal branches of sciatic nerve simultaneously: afferent signals generated from both the lengthened gastrocnemius muscle and the restrained antagonistic muscles were recorded. Remarkably, imposing passive stretch resulted in a significant increase in the firing rates of the units of not only the lengthened muscle, but also of the restrained antagonists ($p < 0,05$ $n=12$). This novel finding suggests that due to epimuscular myofascial force transmission, stretching of the target muscle causes local length changes sensed by the sensory organs within the fibers of the antagonistic muscles, despite being restrained. Our results therefore provide a preliminary support to our hypothesis and are likely to have major implications on our understanding of the functioning of muscular mechanoreceptors.

Keywords: myofascial force transmission, muscle mechanoreceptors, extracellular afferent recordings.

ÖZET

EPİMÜSKÜLER MİYobağDOKUSAL KUVVET İLETİMİNİN DUYUSAL SEVİYEDEKİ ETKİLERİNİN KURBAĞA ALT BACAĞINDAKİ KASLARA AİT AFERENT İŞARETLER İLE DENEYSEL OLARAK İNCELENMESİ

Tendon olmayan yapıların da kuvvet iletiminde başlıca bir rolü olduğunu gösterilmiştir. Epimüsküler miyobağdokusal kuvvet iletimi olarak adlandırılan bu kuvvet iletim mekanizmasının kas fiberleri üzerinde önemli gerinim dağılımlarına neden olduğu dolayısıyla kas fiberleri üzerindeki seri sarkomerlerin boylarında heterojenlik olduğuna dair bulgular mevcuttur. Son çalışmalar antagonist kaslar arasında da epimüsküler miyobağdokusal kuvvet iletiminin önemli ölçüde etkili olduğuna dair bulgular sunmaktadır. Bu çalışmada epimüsküler miyobağdokusal kuvvet iletiminin kas mekanoreseptörlerinde oluşan sinirsel cevabı etkilediği hipotezi kurbağa alt bacağındaki kaslara ait mekanoreseptörlerden kaydedilen duyuşal işaretler ile test edilmiştir. Kurbağa (*Rana ridibunda*) gastroknemiusu distal tendonu kesilip bir makara düzeneği ile 1-5 mm çekilerek uzatılmıştır. Bilek ve diz açıları sırasıyla 100 ve 120 derecede sabit tutulup siyatik sinirin hem tibial hem de peroneal kolundan duyuşal kayıtlar alınmıştır. Bu kayıtlar sırasıyla pasif olarak boyu uzatılan gastroknemius ve boyu sabit antagonist grup mekanoreseptörlerine aittir. Dikkate değer biçimde pasif çekme, boyu uzatılan kasın yanı sıra boyu sabit antagonistlerin aktivitesinde de anlamlı bir artışa neden oldu ($p < 0.05$, $n=12$). Bu yeni bulgu hedef kasa uygulanan çekmenin epimüsküler miyobağdokusal kuvvet iletimi sonucu boyu sabit antagonistte yerel boy değişimleri meydana getirdiğine ve bu değişimlerin antagoniste ait reseptörler tarafından algılandığına işaret etmektedir. Sonuçlar hipotezi desteklemekte ve kas mekanoreseptörlerinin işlevlerini daha iyi anlama doğrultusunda önemli çıkarımlara olanak vermektedir.

Anahtar Sözcükler: miyobağdokusal kuvvet iletimi, kas mekanoreseptörleri, hücre dışı duyu siniri kayıtları.

TABLE OF CONTENTS

ACKNOWLEDGMENTS	iii
ABSTRACT	v
ÖZET	vi
LIST OF FIGURES	ix
LIST OF TABLES	xi
LIST OF ABBREVIATIONS	xii
1. INTRODUCTION	1
1.1 Background	1
1.2 Skeletal Muscle	2
1.2.1 General Structure	2
1.2.2 Muscle Fiber	2
1.3 Force Transmission in Muscle	4
1.3.1 Myotendinous Force Transmission	4
1.3.2 Myofascial Force Transmission	5
1.4 Muscle Mechanoreceptors	7
1.4.1 Muscle Spindles	7
1.4.2 Golgi Tendon Organs	8
1.5 Anatomy of Frog Lower Leg	9
1.6 Objective of the Study	10
2. MATERIALS AND METHODS	11
2.1 Materials	11
2.1.1 Animals	11
2.1.2 Experimental Set-Up and Auxiliary Tools	11
2.2 Methods	12
2.2.1 Preperation	12
2.2.2 Nerve Dissection	13
2.2.3 Stimulus	14
2.2.4 Recordings	14
2.2.5 Off-line Data Analysis	15

2.2.6	Statistics	15
3.	RESULTS	16
3.1	Displacement versus Load on Muscle	16
3.2	Effects of Stretch of a Target Muscle on Its Antagonists	16
3.3	Effects of Different Stretch Amplitudes	18
4.	DISCUSSION	20
4.1	Effects of Passive Stretch	20
4.2	Changes in Response with Different Stretch Amplitude	20
4.3	Limitations of the Study	21
	APPENDIX A. MATLAB CODE FOR SINGLE UNIT SPIKE SORTING	23
	REFERENCES	26

LIST OF FIGURES

Figure 1.1	Schematic diagram of the structural organization of the skeletal muscle (top), and the individual muscle fiber (bottom) [2].	2
Figure 1.2	Electron microscope image of a single sarcomere and part of its neighbor sarcomeres (A) and, schematic representation (B) [4].	3
Figure 1.3	Active length tension curve of an individual sarcomere [1].	4
Figure 1.4	A generalized passive length-tension curve (A), and total length-tension curve for a typical isolated muscle (B) [2].	4
Figure 1.5	Schematic view of connecting proteins allowing lateral transmission of force across the sarcolemma [3].	5
Figure 1.6	Scanning electron micrograph of the endomysial connective tissue within skeletal muscle [11].	6
Figure 1.7	A mammalian muscle spindle, the structure shown here is encapsulated with a fusiform sphere, much like the one in frog (a) and a frog muscle spindle (b) [3, 18].	7
Figure 1.8	Response of a muscle spindle afferent to active contraction (top) and passive sinusoidal vibrations superimposed on it [21].	8
Figure 1.9	GTO structure (a), GTO has been dissected and the capsule surrounding it removed, remaining section was zoomed in. The collagen and the nerve fibers are intertwined (b) [3].	9
Figure 1.10	Response of a GTO afferent to active contraction (top) and passive sinusoidal vibrations superimposed on it [21].	9
Figure 1.11	Cross section of the frog lower leg (A), and the innervation map of frog leg (B) [22].	9
Figure 2.1	Schematic representation of the experimental set-up	11
Figure 2.2	Signal obtained by window discriminator (top) versus raw signal in digital form (bottom).	15
Figure 2.3	Off-line analysis for detecting spikes from single units.	15
Figure 3.1	Off-line analysis for detecting spikes from single units.	16

Figure 3.2	Instantaneous frequencies versus time for recording from tibial nerve branch innervating stretched gastrocnemius, stretch amplitude=2mm.	17
Figure 3.3	Instantaneous frequencies versus time for recording from peroneal nerve branch innervating restrained antagonists, stretch amplitude=2mm.	17
Figure 3.4	Relationship between amount of gastrocnemius stretch and firing rate for gastrocnemius muscle.	18
Figure 3.5	Relationship between amount of gastrocnemius stretch and firing rate for lengthwise restrained antagonist muscle.	19
Figure 4.1	Intermuscular connections transmit force on gastrocnemius muscle caused by stretch.	20
Figure 4.2	Spike rate at different lengths for individual gastrocnemius afferent units.	21
Figure 4.3	Spike rate at different lengths for individual antagonist afferent units.	21

LIST OF TABLES

Table 1.1	Differences of mammalian and frog muscle spindles.	8
Table 3.1	Average number of spikes during steady state of each exeperiment for recordings from the tibial branch (gastrocnemius).	18
Table 3.2	Average number of spikes during steady state of each exeperiment for recordings from the peroneal branch (restrained antagonists).	18

LIST OF ABBREVIATIONS

MFT	Myofascial Force Transmission
GTO	Golgi Tendon Organs
CNS	Central Nervous System
EDL	Extensor Digitorum Longus muscle
TA	Tibialis Anterior muscle
EHL	Extensor Hallucis Longus muscle

1. INTRODUCTION

1.1 Background

Execution of controlled bodily movements in higher organisms is realized by the activity of skeletal muscles. This requires;

1. forces generated by muscles and moments resulting from that force applied to joints
2. a control circuit to monitor these forces and the changes they yield, and make the necessary adjustments.

Forces can be active; generated by specialized structures within the muscle upon neural stimulation, or passive; resulting from sources other than stimulated muscle such as resistance of the muscular and connective tissue to stretch. Transmission of force can be at specialized locations where the muscle fuses with the bone; the myotendinous way or lateral transmission via connective tissue structures can occur; the myofascial way. Motor neurons of the CNS innervate the skeletal muscle and carry the stimulus for active contraction. The intensity of the contraction is dependant on muscles current state. In terms of control, the information about the state of muscle is constantly fed into the central nervous system via specialized structures within the muscle. Muscle spindles and Golgi tendon organs are two most prominent receptor types, signaling the length and tension changes respectively.

1.2 Skeletal Muscle

1.2.1 General Structure

Muscle is a visco-elastic tissue of the body which is primarily responsible for generation of force to produce movement. Skeletal muscle, to which locomotion and posture is attributed, is distinguished from other types of muscles in the body (namely smooth muscle and cardiac muscle) by voluntary contraction and striated appearance under light microscope [1].

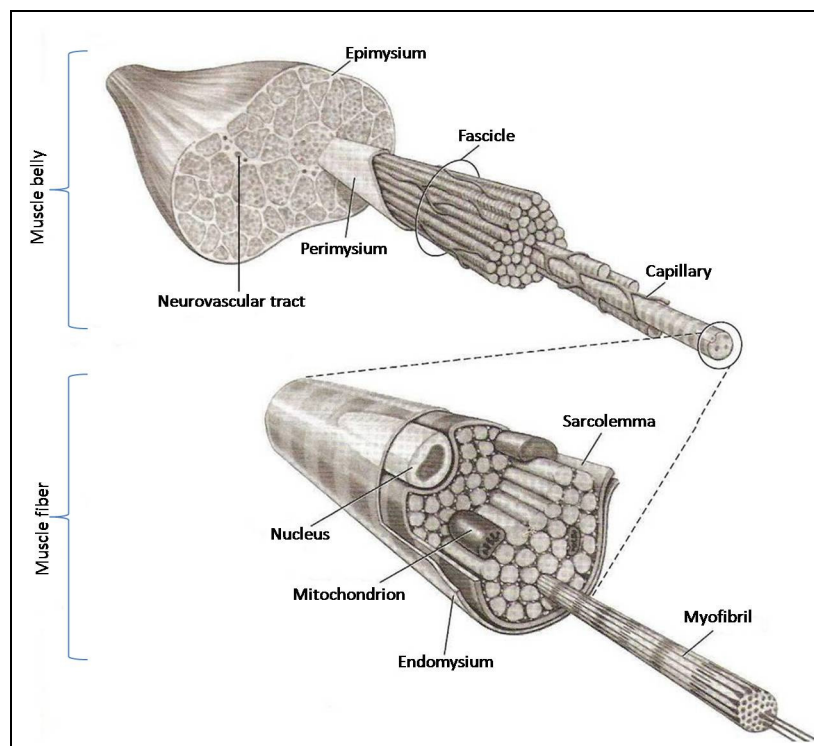


Figure 1.1 Schematic diagram of the structural organization of the skeletal muscle (top), and the individual muscle fiber (bottom) [2].

There is a hierarchical organization in skeletal muscle structure (see Figure 1.1). Three structurally related sets of connective tissue exist, dividing the muscle in different yet interconnected compartments: **epimysium**, **perimysium** and **endomysium**.

Epimysium surrounds the entire surface of the muscle and determines the border by separating it from other muscles. The epimysium contains tightly woven bundles

of collagen fibers that are highly resistive to stretch. The *perimysium* lies beneath the epimysium and divides the muscle into compartments known as the fascicles. In the space between the fascicles nerves and blood vessels, collectively known as neurovascular tract, run and maintain blood flow and innervation of the muscle tissue. The *endomysium* encloses the individual muscle fiber. It is composed of a relatively dense meshwork of collagen fibrils which connect to the endomysia of neighboring muscle fibers [2, 3].

1.2.2 Muscle Fiber

A single muscle cell is called a *muscle fiber* (see Figure 1.1). Highly specialized for rapid and efficient contraction, this long, thin muscle fibers form during development of the organism by fusion of many separate cells and therefore retains many nuclei. In every muscle fiber there are several hundred to several thousand *myofibrils*, which are cylindrical structures with 1-2 μm in diameter and they make up for the majority of the muscle cell cytoplasm (a.k.a. sarcoplasm) [4].

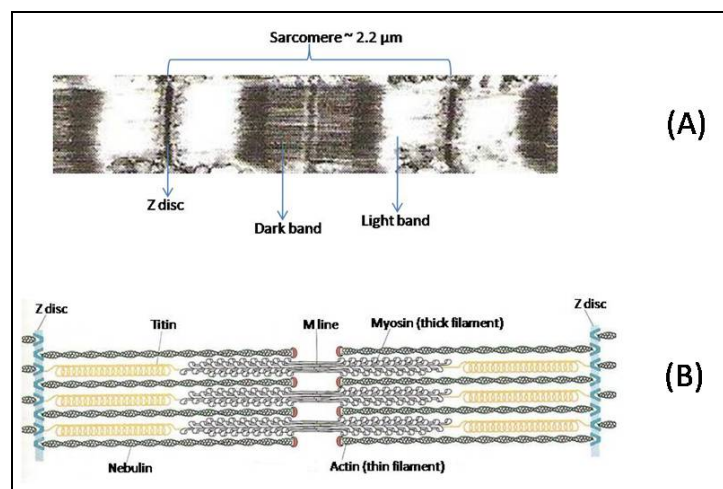


Figure 1.2 Electron microscope image of a single sarcomere and part of its neighbor sarcomeres (A) and, schematic representation (B) [4].

Each myofibril is a serial array of sarcomeres (see Figure 1.2). *Sarcomeres* are the smallest contractile elements of the muscle which give the myofibrils their striated appearance [2, 4]. Each sarcomere contains thin and thick filaments that partially

overlap. Main component of the thin filament is the actin protein and it is attached to the Z disc at each end of the sarcomere. Thick filament is comprised of myosin. There are several other proteins in this assembly. Titin is a spring-like protein running from Z disc to M line serving as a binding site for myosin. Nebulin serves as a template for the thin filament and stretches along its length.

Active force generation is described by the sliding filament hypothesis [5, 6]. In an ATP driven process the myosin heads slide over the thin filaments, attach their heads to the actin molecule and form cross-bridges thereby shorten the length of the sarcomere without changing the lengths of individual filaments. Active force in muscle is the summation of these forces between cross-bridges throughout the sarcomeres of the whole muscle.

As a consequence of the typical arrangement of the filaments in a sarcomere, the force generating capability is associated with its instantaneous length. Figure 1.3 shows the length-force characteristics of a sarcomere along with relative positions of actin and myosin filaments at a given instant. At extremely long lengths there are not enough cross bridges and at extreme low lengths the thick filaments overlap, again decreasing the number of cross bridges effective in force generation. There is an optimum length for a sarcomere where it reaches its maximum number of cross bridges therefore producing maximum amounts of force.

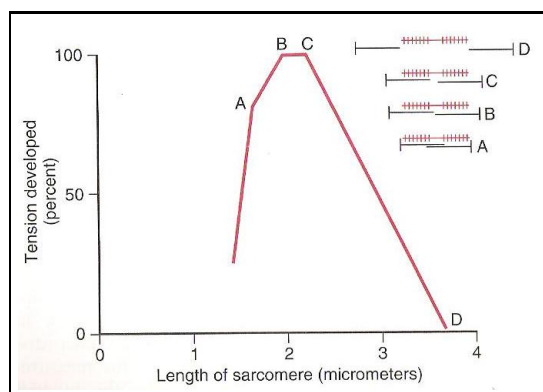


Figure 1.3 Active length tension curve of an individual sarcomere [1].

1.3 Force Transmission in Muscle

Figure 1.4 shows the length force characteristic of an isolated muscle. There are mainly two components of the overall length-force curve. The active component is similar to the length-tension curve of a single sarcomere. This is because it is essentially the summation of the behavior of many sarcomeres. The passive component is mainly due to muscle's stiffness. Both non-muscular such as connective tissue and tendon and muscular structures (i.e. myofibers) yield resistance to external and internal effects such as gravity and stretch.

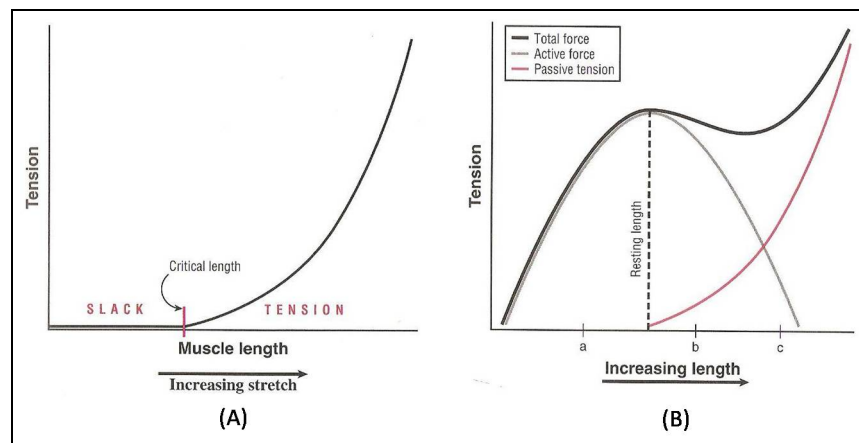


Figure 1.4 A generalized passive length-tension curve (A), and total length-tension curve for a typical isolated muscle (B) [2].

Posture and aimed locomotion are result of either balance of these forces or imbalance of them. In any case transmission of muscular force to skeletal structures is required. Two major mechanisms have been identified: i) Transmission at the site where muscle fibers fuse with the tendinous structures; *myotendinous force transmission*; ii) Transmission of force laterally via multi-molecular connections between the muscle fibers and the extracellular matrix along the full periphery; *myofascial force transmission*.

1.3.1 Myotendinous Force Transmission

Myotendinous force transmission implies force generated by myofibers is transferred to tendons and from there on to the skeleton [7]. Unique mechanical properties of the tendon are supporting observations in favor of myotendinous force transmission: Muscle fibers decrease in diameter by nearly 90% as they fuse with the tendon tissue thereby increasing force per cross-sectional area per fiber by a considerable amount [8]. Towards both origin and insertion ends of a muscle fiber, extensive foldings of the sarcolemma make invaginations into the myofibers, seemingly serving to disperse the force to a larger area at that region [2, 7]. Furthermore, longitudinal orientation and thickness of the collagen fibers of the tendon [2] and identification of putative attachment proteins such as talin, paxilin and tensin at the fusion zone [3] are findings in favor of myotendinous force transmission.

Myotendinous force transmission has been held as the exclusive channel for force transmission. Forces at both ends of a muscle, which is isolated from its neighboring muscles and connective tissue structures, are equal. Repeated observation of this situation might have led to the belief that muscle fibers transmit their force only in longitudinal direction (i.e. in series) only. However muscle is not an isolated entity in its natural environment within the body. It has been shown mechanisms other than myotendinous pathways play substantial role in muscle force transmission (see [7] and [9] for review).

1.3.2 Myofascial Force Transmission

In addition to connections at myotendinous sites where the muscle fiber meets the tendons at both ends, myofibers are also connected to extracellular space by transsarcolemmal proteins all along the length of the fiber. Outside the sarcolemma of each muscle fiber is extracellular matrix made up of proteins and connective tissue material in continuity with the endomysium. Experiments with a single fiber isolated from frog muscle demonstrated that force generated by myofibrils can be transmitted solely via

sarcolemma-endomysium complex along the fiber [10].

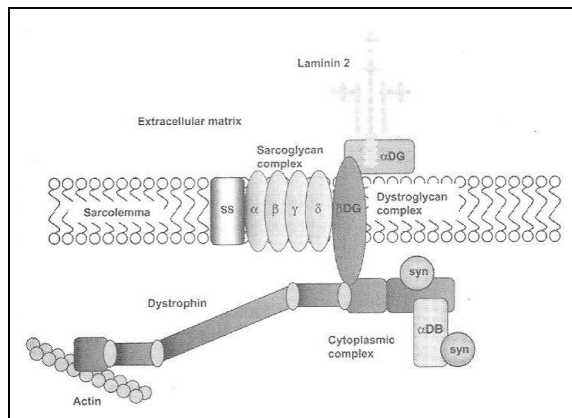


Figure 1.5 Schematic view of connecting proteins allowing lateral transmission of force across the sarcolemma [3].

Moreover, in its natural environment (i.e. in vivo conditions) a skeletal muscle is part of an integral system rather than an independent entity. It is connected to other muscles directly via collagenous linkages between the epimysial structures. In addition to such intermuscular connections, compartmental boundaries and the neurovascular tract also serve to the continuity of muscular and non-muscular structures at locations other than the tendon origin and insertion. It has been shown that those epimuscular connections serve as an important alternative to myotendinous pathway in force transmission and the term epimuscular myofascial force transmission has been coined [7]. Myofascial force transmission can be further classified on basis of which myofascial structures provide major contribution to force transmission process:

1. *Intramuscular myofascial force transmission*: Previously described three layers of connective tissue are interwoven as a continuous sheet rather than being separate entities. In that sense skeletal muscle can be considered as a three dimensional system of endomysial tunnels in which the muscle fibers operate [11] (see Figure 1.6). This network of tunnels provides pathways for muscular force produced at the fibers to be transmitted throughout the whole muscle belly. Such transmission is referred to as intramuscular myofascial force transmission [7]. There is experimental work showing that this type of force transmission can bear a substantial amount of a muscle's overall force transmission activity even in the

absence of myotendinous connections [12].

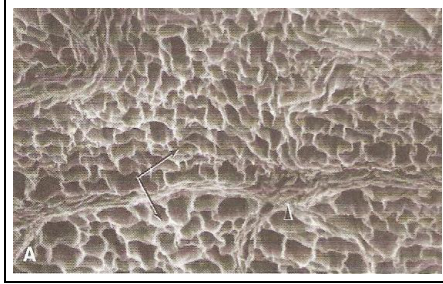


Figure 1.6 Scanning electron micrograph of the endomysial connective tissue within skeletal muscle [11].

2. *Intermuscular myofascial force transmission*: There are direct collagenous connections between the epimysia of neighboring muscles. As a consequence, the intramuscular myofascia of adjacent muscles are continuous. Force transmission between muscles by means of their epimysia is termed intermuscular myofascial force transmission [13, 14].
3. *Extramuscular myofascial force transmission*: Structures that make up the neurovascular tract (i.e. blood vessels, nerves and other support tissues) also provide means of transmission for muscular force [15, 16].

Above mentioned, collectively known as *epimuscular myofascial force transmission* has several substantial effects on muscular biomechanics. Two of them are: 1) The forces exerted at the origin and insertion of a muscle are unequal. Studies on rat EDL muscle with intact neighboring structures revealed proximo-distal force difference is a function of the length in which the muscle operates and its relative position to surrounding muscles [14, 17]. 2) The lengths of sarcomeres within a muscle are not homogenous. Continuous network of intra- and intermuscular connective tissue throughout musculoskeletal system result in a heterogeneous distribution of myofascial loads along the muscle fiber and cause unequal sarcomere lengths along the fiber [15].

1.4 Muscle Mechanoreceptors

1.4.1 Muscle Spindles

Muscle spindles are sensory organs that monitor the length of a muscle as well as its rate of change of length [3]. The structure called spindle is a capsule filled with interstitial fluid, size of capsule being variable of subject organism or muscle. Common to all muscle spindles, a special type of muscle fiber called the intrafusal muscle fiber is present in the capsule. There is both efferent and afferent innervation to these fibers and they are devoid of myofibrils at the equator region. The spindles are surrounded by, and are situated in parallel with, the extrafusal muscle fibers that constitute most of what is called a muscle belly.

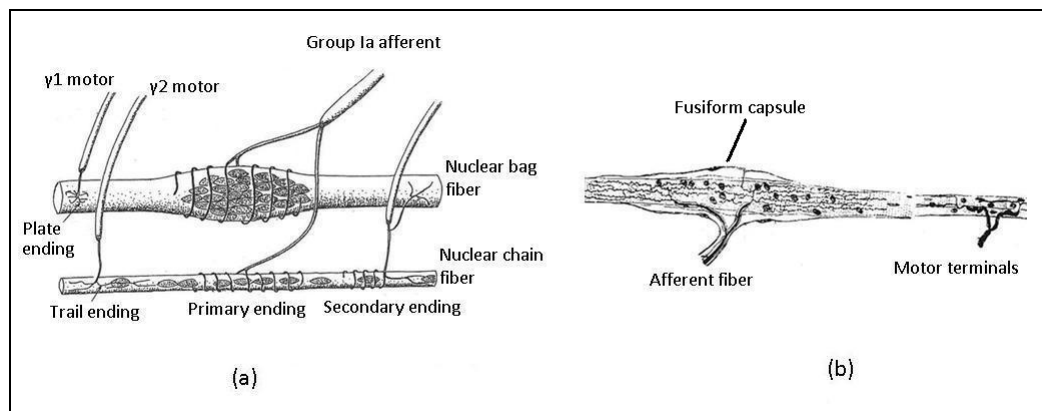


Figure 1.7 A mammalian muscle spindle, the structure shown here is encapsulated with a fusiform sphere, much like the one in frog (a) and a frog muscle spindle (b) [3, 18].

When a muscle stretches, thereby increases length, these extrafusal fibers squeeze the capsule that the intrafusal fibers are in and result in afferent response [18]. It should be noted that there are some structural (and potentially functional) differences between the amphibian and mammalian muscle spindle (see Table 1.1).

Different stimulus types have been used to identify muscle spindles' response characteristics. These include combinations of ramp-and-hold, sinusoidal and active contraction. In a broad sense behavior of muscle spindle to a particular stimulus is such: In a ramp and hold stretch there's no or very low discharge during the pre-ramp

Table 1.1
Differences of mammalian and frog muscle spindles.

Mammalian	Amphibian
Two or more sensory fibers	One sensory fiber only
Two distinct types of intrafusal fibers	No clear distinction between individual intrafusal fibers
Few mm long, usually shorter than the muscle that it is embedded	Intrafusal fiber runs from tendon to tendon
One sensory region only	Sensory regions arranged in series

stage. Upon stretch the receptor the receptor fires at a frequency proportional to the amplitude of stretch. In the steady phase adaptation occurs and firing rate is somewhat lower than the rising phase [19, 20]. Figure 1.6 shows response of a muscle spindle afferent taken from frog's biceps muscle afferents during active contraction. Pause in firing is a characteristic of muscle spindles and is used to distinguish them from tension receptors [21]. When a passive stimulus such as stretch or sinusoidal vibration as in lower chart in Figure 1.8 is given spindle activity increases in correlation with the stimulus amplitude and frequency.

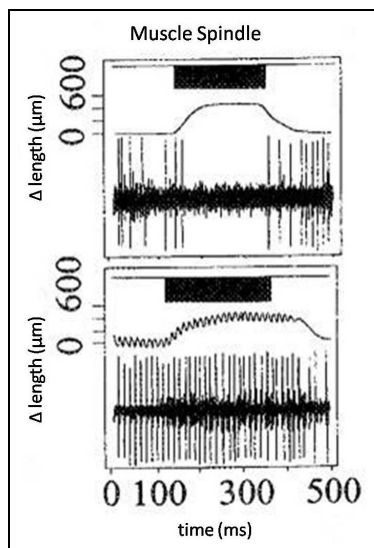


Figure 1.8 Response of a muscle spindle afferent to active contraction (top) and passive sinusoidal vibrations superimposed on it [21].

1.4.2 Golgi Tendon Organs

Golgi tendon organs are located at the myotendinous junction rather than the belly. GTO is a specialized structure where fine nerve fibers are interspersed in collagen bundles of the myotendinous junction. In that sense they lie 'in series' with the muscle fibers and when the muscle fibers contract the collagen bundles straighten and compress the nerve thereby setting up impulse discharges [3].

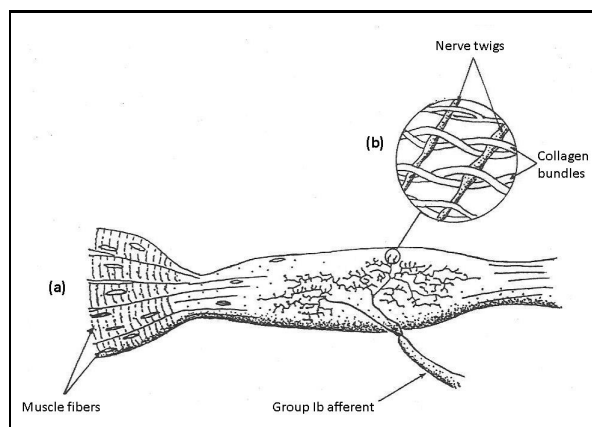


Figure 1.9 GTO structure (a), GTO has been dissected and the capsule surrounding it removed, remaining section was zoomed in. The collagen and the nerve fibers are intertwined (b) [3].

Figure 1.10 summarizes their general response characteristics. GTOs are distinguished by increase in their firing rate during active contraction. Firing is more frequent during rising phase of the contraction. GTOs respond to passive stretch too, though they are known for having a higher threshold to passive stretch compared to spindles [21].

1.5 Anatomy of Frog Lower Leg

Calf portion of frog lower leg is comprised of tibialis posticus and gastrocnemius, which constitute a big portion of total muscle mass. There are four muscles in the extensor aspect: peroneous, tibialis anticus, extensor cruris and flexor tarsi anterior. These two groups work as antagonists. Towards the distal third of the thigh, the sciatic nerve splits into two main branches, namely 'nervus peroneus' (peroneal nerve) and

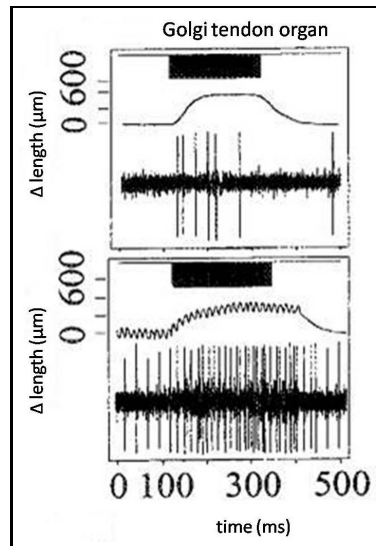


Figure 1.10 Response of a GTO afferent to active contraction (top) and passive sinusoidal vibrations superimposed on it [21].

'nervus tibialis' (tibial nerve). It was established that calf muscles are innervated by the tibial nerve whereas the antagonist group is innervated by the peroneal nerve [22].

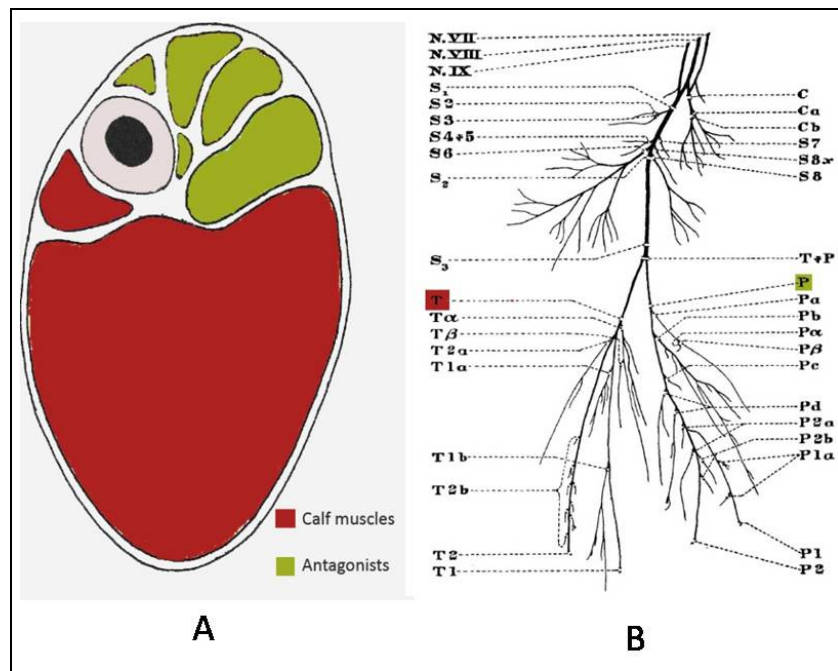


Figure 1.11 Cross section of the frog lower leg (A), and the innervation map of frog leg (B) [22].

1.6 Objective of the Study

Previously it has been suggested that myofascial force transmission might have implications on the activity of sensory organs of the muscle, as well as muscular biomechanics. It has been proposed most likely owing to the proximo-distal force differences, different Golgi tendon organs at the proximal and distal ends of a muscle would respond accordingly, thereby acting as sensors of proximo-distal force differences. With the same line of thought, functions of muscle spindles may be redefined to include their role as sensors for detecting the local stress distributions on the fiber they are located [16].

In this work, it is hypothesized that epimuscular myofascial loads acting on lengthwise restrained antagonists imposed by changing lengths of gastrocnemius, to which they are connected via myofascial connections only, would evoke sensory response recorded from that muscle group. In order to test this hypothesis gastrocnemius of frog lower leg was given passive ramp-and-hold and meanwhile sensory activity of the lengthwise restrained antagonist muscles was recorded.

2. MATERIALS AND METHODS

2.1 Materials

2.1.1 Animals

37 common water frogs (*Rana ridibunda*) of either sex, weighing between 24 to 51 grams, were used. The frogs were kept in a glass pool, with 12h light/dark cycles and fed with live grasshoppers. Experimental protocols were in agreement with the guidelines and regulations concerning animal welfare and experimentation set forth by Turkish law, and approved by the Committee on Ethics of Animal Experimentation at Boğaziçi University.

2.1.2 Experimental Set-Up and Auxiliary Tools

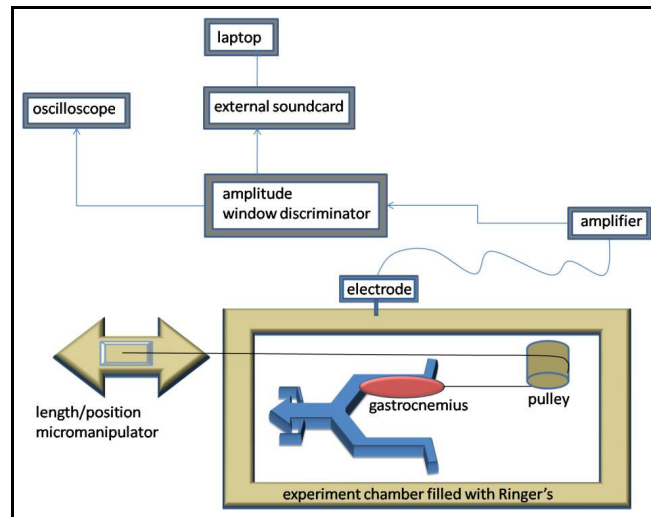


Figure 2.1 Schematic representation of the experimental set-up

- Common surgical tools such as forceps, scissors and scalpel were used for the animal preparation. Cut tendon of the gastrocnemius muscle was tied to the length/position manipulator with Kevlar thread.

- Standard Ringer's solution was prepared in order to prevent muscle and nerve tissue from drying throughout the experiment. The formulation of the solution is as such: (112 mM *NaCl*, 1.9 mM *KCl*, 1.1 mM *CaCl*₂, 1.1 mM *Glucose*, 2.4 mM *NaHCO*₃, and 1.0 mM *NaH*₂*PO*₄ [23]).
- A pH-meter was utilized to keep record of the solution before and after the experiment. For all experiments pH was never out of 6.4 - 6.8 interval.
- Ambient temperature was measured before and after the experiment. The temperature remained in-between 23.4-25.6 °C at all times.
- Previous studies established [24, 25] platinum has superior signal-to-noise characteristics compared to the other available alternatives tungsten and aluminum. Thus a platinum hook electrode attached to a micromanipulator was used for recordings.
- An Alan key was mounted to the knob of the position/length micromanipulator and that assembly served for giving the ramp-and-hold stretch to the muscle. One full counter-clockwise rotation of the key corresponded to 1 mm of lengthening and one full clockwise rotation to 1 mm of shortening.
- A custom made amplifier was used for recording the afferent signals. Spikes were 10000 times amplified before reaching the discriminator and the soundcard.
- An amplitude window discriminator was connected to the output of the amplifier in order to select for single units. This window discriminator was later bypassed and the whole signal was analyzed off-line with a custom MATLAB code.
- An external sound-card received the signals coming from the discriminator and the spike data was saved as a .wav file in a laptop to be analyzed later.

2.2 Methods

2.2.1 Preperation

Frogs were cold-anesthetized in $-4^{\circ}C$ for approximately 5 minutes. They were double-pithed afterwards. Skin of the leg to be studied was completely removed. At this point the leg was arranged so that the hip, knee and ankle angles were 120° , 120° , 100° respectively and keeping that conformation the animal was fixed on the wax base of the experimental chamber using bone pins. The position of the Achilles tendon was noted at this point for reference. Achilles tendon was cut as distal as possible. The flap at the end of the loose end of the tendon is passed through a loop formed by Kevlar thread. The flap is then folded onto itself and three securing knots were made with special surgical threads so that the tendon is fixed tightly and wouldn't loosen upon stretch at some point during the experiment. The other end of the Kevlar thread is directed out of the experiment chamber via a pulley mechanism and is securely tied to the length/position manipulator (see Figure 2.1). The chamber is filled with previously prepared standard Ringer's solution.

2.2.2 Nerve Dissection

The fascia connecting the thigh muscles was removed and the sciatic nerve was exposed. The nerve was cut slightly above the bifurcation point, where the tibial (thicker) and peroneal (thinner) branches were distinguishable. Cutting provided easy access to both branches for dissection and isolation of any feedback loops of the spinal cord during the recording. The freed branch (either tibial or peroneal depending on which muscle's afferents are targeted) was placed on a thin plastic stratum which is fixed to the wax by needles. Under light microscope stepwise dissection was applied to the nerve branch [26]. This is done as follows: First the main branch is separated resulting in two fibers. Each of these fibers is then placed on the electrode and checked for existence of muscle afferent fibers. Two types of stimuli, palpation of muscle at several regions with Von Frey filaments and passive stretch, were given to check for

existence. Meanwhile the signals were monitored both from the oscilloscope screen and the speakers. The fiber having more frequent firing during the stretch stimulus is kept for further dissection. If spikes are more prominent during palpation, then the fiber is assumed to convey more from freed tactile ends upon skinning rather than muscle proprioceptive afferents and that fiber is left out. This stepwise manner was repeated until the nerve fiber was as fine as the dissecting needle can separate.

2.2.3 Stimulus

At the end of the dissection, the standing out fiber is placed on the hook electrode and gastrocnemius muscle was brought to reference length. The recording started 10 seconds prior to ramp. At the 10th second on metronome click, ramp was given manually by revolving the Alan key mounted to the knob of the position/length manipulator. It was always 1 revolution per second up until the predetermined extension was reached, i.e. 2 revolutions for 2 mm, 3 revolutions for 3 mm and so forth. At the end of stretch muscle was kept at that final length for 20 more seconds and then released. There was 1 minute of intermission between subsequent recordings. In two experiments load on muscle was also recorded by mounting force transducer on top of the position manipulator. Similar values of force indicated equal amounts of load on each try therefore this procedure was not repeated for all experiments.

2.2.4 Recordings

Preliminary stimuli were given and output was observed on the oscilloscope screen. Meanwhile the output from the both the discriminator and the oscilloscope is recorded on the laptop as a .wav file thorough the external soundcard. Sampling rates were always higher than 11 kHz to ensure no data is lost. Figure 2.2 is an example how recordings in two channels look like. Both discriminated and raw signals were recorded via two separate channels of the soundcard. However it turned out that working with raw data and applying off-line analysis to it is more favorable due to following reasons:

1. There were discrepancies between spikes observed in raw data and output from the discriminator. There were missed events falling within the window aperture and yet not recorded by the discriminator (Figure 2.2)
2. It was possible to apply different window apertures to the same recording therefore allowing for selection of different units. This is not practical to do using the discriminator.

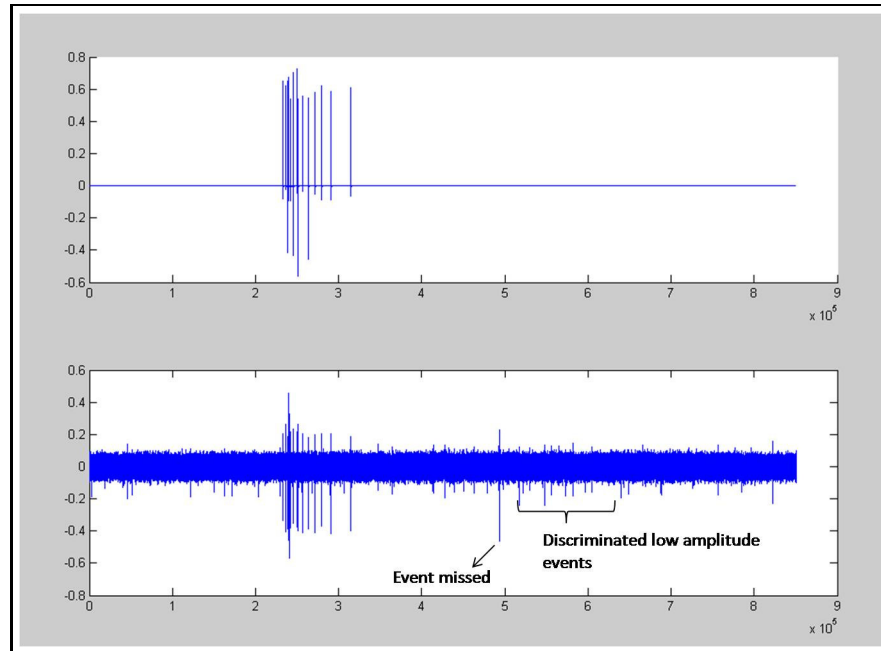


Figure 2.2 Signal obtained by window discriminator (top) versus raw signal in digital form (bottom).

2.2.5 Off-line Data Analysis

A custom MATLAB code was used for off-line analysis (see APPENDIX). The raw data is plotted and after the data is visually observed the user is asked to select a desired window that would select for a single unit of interest. Individual spike times for that unit are then saved for further analysis. Individual spike times are used to calculate instantaneous frequencies (inverse of inter-spike interval) and number of spikes per a time interval (e.g. spikes/seconds) during different phases of the recording.

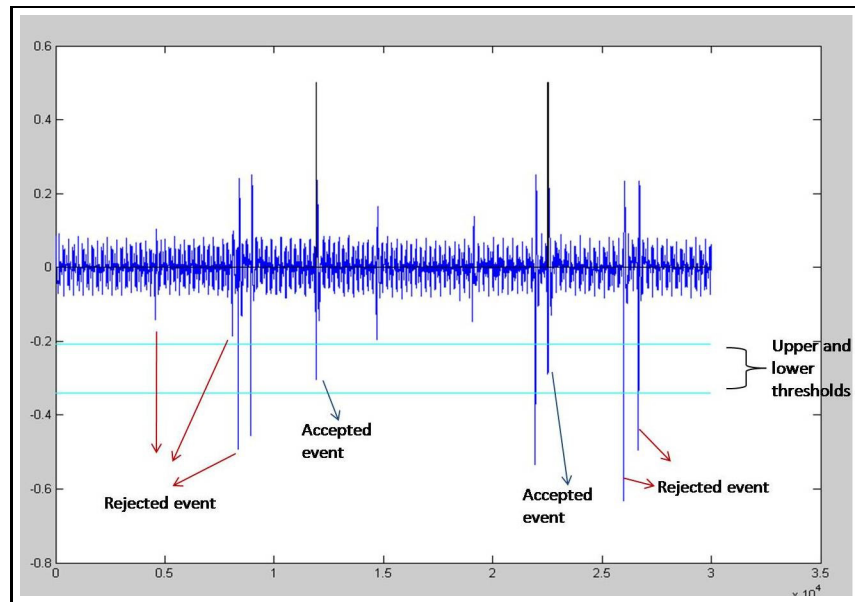


Figure 2.3 Off-line analysis for detecting spikes from single units.

2.2.6 Statistics

Statistics was applied to see whether the effect of stretch amplitude over firing rate is significant. Response during the steady-state was used (i.e. between 16-25 seconds). Each data column, corresponding to a particular stretch amplitude, contained average number of spikes for each experiment and these columns were tested to see whether they belong to a normal distribution using functions like 'kstest' and 'lillietest' in MATLAB Statistics toolbox. However some columns in both nerves failed to pass for normalcy, therefore non-parametric testing was applied to the whole data set.

3. RESULTS

The following data are presented in this chapter: a) Load on gastrocnemius muscle caused by ramp-and-hold stretch, b) Instantaneous frequency charts and time histograms with 1 second bin size from both nerves, and stretch amplitude versus firing rate obtained from c) 13 recordings from the tibial branch and d) 12 recordings from peroneal branch.

3.1 Displacement versus Load on Muscle

Force measurements taken from the transducer connected to gastrocnemius muscle during stretches is as shown in Figure 3.1.

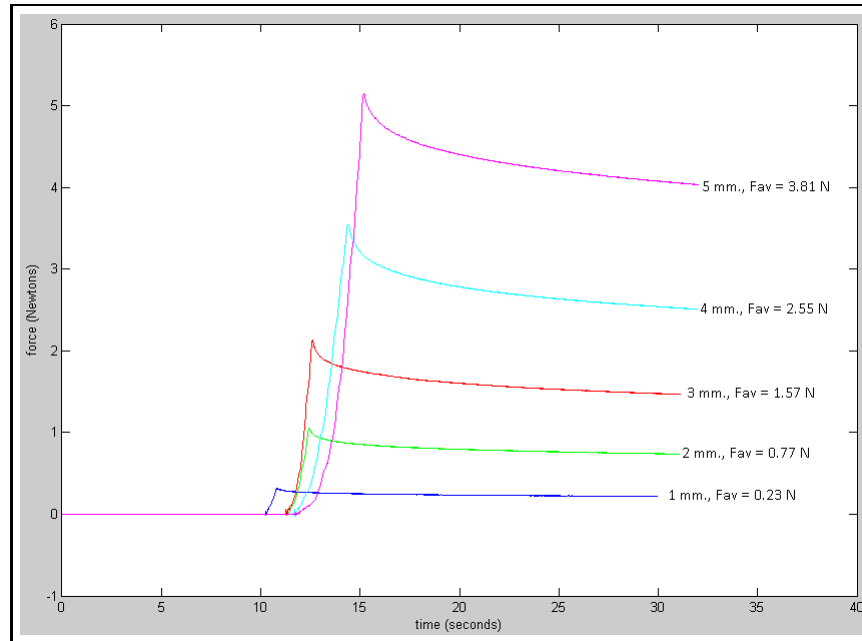


Figure 3.1 Off-line analysis for detecting spikes from single units.

A force value for a given stretch reaches its peak value at the end of the ramp and due to material properties of muscle the force is not constant during maintained stretch. In order to calculate the average force acting on the muscle for each stretch after the ramp phase, points to the right of the peak value of each curve were averaged.

Values obtained this way are 0.23 N, 0.77 N, 1.57 N, 2.55 N and 3.81 N for 1 mm, 2 mm, 3 mm, 4 mm and 5 mm of stretch amplitudes respectively. Therefore we conclude that for all stretches, thresholds for both muscle spindles and GTOs are crossed [27, 28], indicating that responses might have come from either of those two receptor types.

3.2 Effects of Stretch of a Target Muscle on Its Antagonists

The change in firing frequency of the recorded afferent during different phases of a stretch amplitude is investigated by calculating the instantaneous frequency. (see Figures 3.2 and 3.3.)

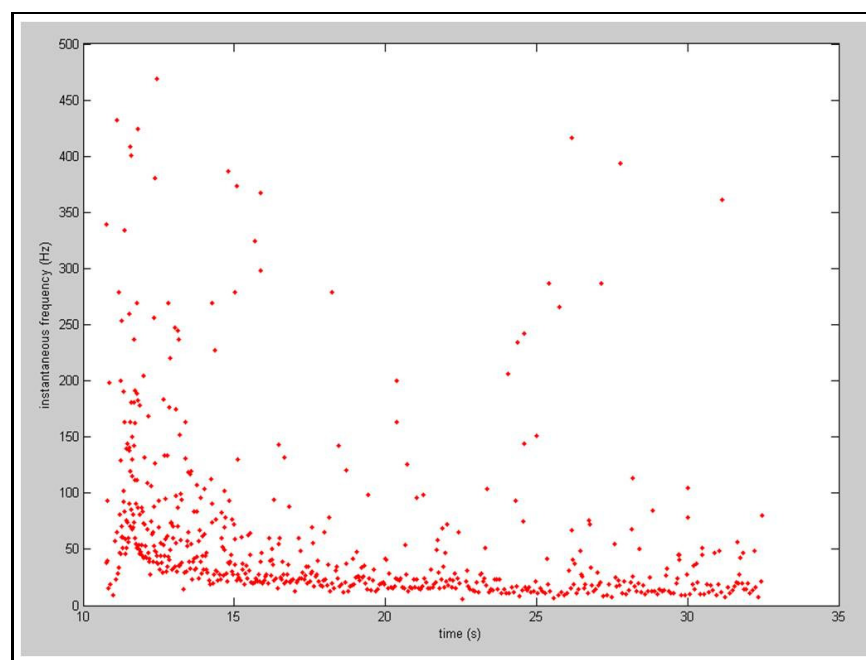


Figure 3.2 Instantaneous frequencies versus time for recording from tibial nerve branch innervating stretched gastrocnemius, stretch amplitude=2mm.

Instantaneous frequency, which is simply the inverse of inter-spike interval, is an indicator of the regularity of a response. The first 10 second belongs to the pre ramp phase, which is relatively silent. The firing rate increases during the ramp phase, reaching to its peak at the end of ramp. In a 2 mm stretch the ramp phase lasts for 2 seconds (i.e. velocity is always 1mm/sec). There is a 20 seconds of maintained stretch period after the ramp which is marked by a gradual drop in the firing rates.

At the end of the maintained stretch period the gastrocnemius muscle is released to its original length and the activity returns to pre-ramp phase. The regularity of the results, of which Figure 3.2 is a special case for 2 mm of stretch, allow us to conclude the response comes from a single unit. Increase in frequency during ramp and a subsequent adaptation during maintained stretch are indicators of that single unit being a muscle spindle [20].

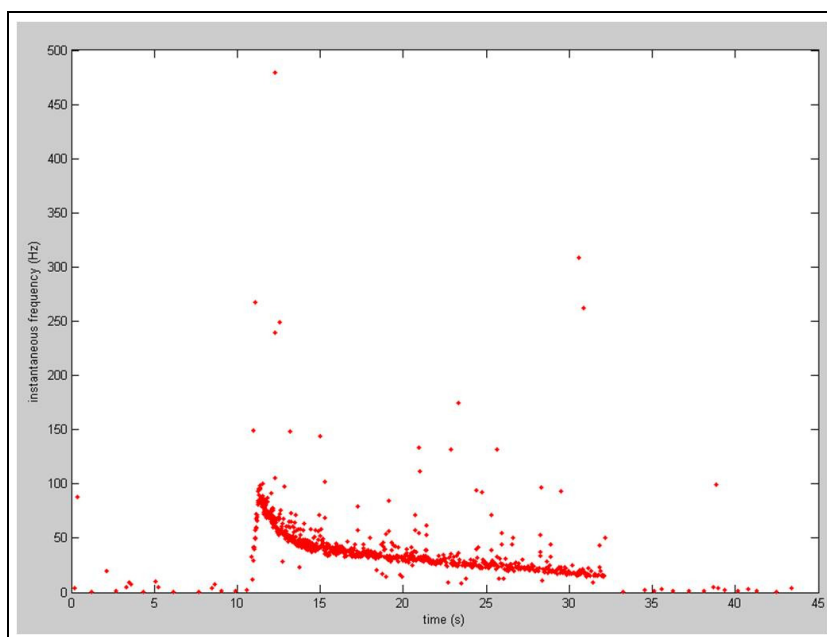


Figure 3.3 Instantaneous frequencies versus time for recording from peroneal nerve branch innervating restrained antagonists, stretch amplitude=2mm.

Figure 3.3 is instantaneous frequency versus time graph for afferents of lengthwise restrained antagonists for 2 mm stretch of gastrocnemius. Remarkably, except for a minor spontaneous activity during pre and post stimulus phases, the behaviour of antagonist afferents is quite similar to gastrocnemius afferents. The results for other stretch amplitudes were also similar in behaviour, only higher frequencies with increasing amounts of stretch. With this results we conclude that imposing passive stretch resulted in an increase in the firing rates of the units of not only the lengthened muscle but also of its lengthwise restrained antagonists.

3.3 Effects of Different Stretch Amplitudes

Average number of spikes per second during the steady state (that is taken as the 10 second long period between the 16th and 25th seconds of each recording) was calculated for both group of recordings. The results are given in Tables 3.1 and 3.2.

Table 3.1

Average number of spikes during steady state of each exeperiment for recordings from the tibial branch (gastrocnemius).

#	1	2	3	4	5	6	7	8	9	10	11	12	13	Median
1	21.4	6.2	1.7	7.3	6.2	2.4	7.3	2.4	2.3	2.3	2.4	5.5	26	5.5
2	52.8	20.5	20.6	37.5	20.1	23.7	37.5	22.9	30.3	29.6	10.5	19.7	53.7	23.7
3	70.5	26.9	60.9	42.9	26.3	62.7	43.3	71.3	53.2	53.4	61.2	25.4	72	53.4
4	67.9	51.4	48.8	42.5	48.6	68.5	48	92.1	58.8	57.6	73.6	48	74.8	57.6
5	75.5	83.9	30	45.5	78.2	64	49	82.2	61.6	60.8	79.9	79.1	77.5	75.5

Table 3.2

Average number of spikes during steady state of each exeperiment for recordings from the peroneal branch (restrained antagonists).

#	1	2	3	4	5	6	7	8	9	10	11	12	Median
1	0	4.8	13.8	27.6	3.6	29.2	26.2	0.1	5.4	21.9	29.3	3.6	9.6
2	0.8	14.8	17	22	32.7	29.8	24.1	0.8	15.1	38.1	39.4	32.1	23.05
3	1.9	19.6	34.3	28.1	37.1	30.7	26.4	1.9	25.7	43.8	36.8	40.5	29.4
4	2.3	31.8	36.6	44.8	20.7	16	39.9	2.3	32.9	51.4	18.2	47.6	32.35
5	3.2	44.3	48.3	40.7	1.8	5.4	43	3.2	49.4	69.5	9.4	58	41.85

The rows of data in Tables 3.1 and 3.2 were tested non-parametrically. Firing rate during steady state was shown to be significantly different with different amounts of stretch ($p=1.84e-9$ for tibial branch and $p=0.0011$ for peroneal branch). The bar charts in Figures 3.4 and 3.5 presents visual indication of a correlation between increasing firing rate and increasing stretch. This was verified with a Spearman correlation test ($p=2.32e-16$ for tibial and $p=0.0059$ for peroneal).

Results in Tables 3.1 - 3.2 and Figures 3.4 - 3.5 allow us to conclude that firing rates differ significantly with different amounts of stretch and they are correlated. The results also serve as a verification of the finding for various stretch amounts that

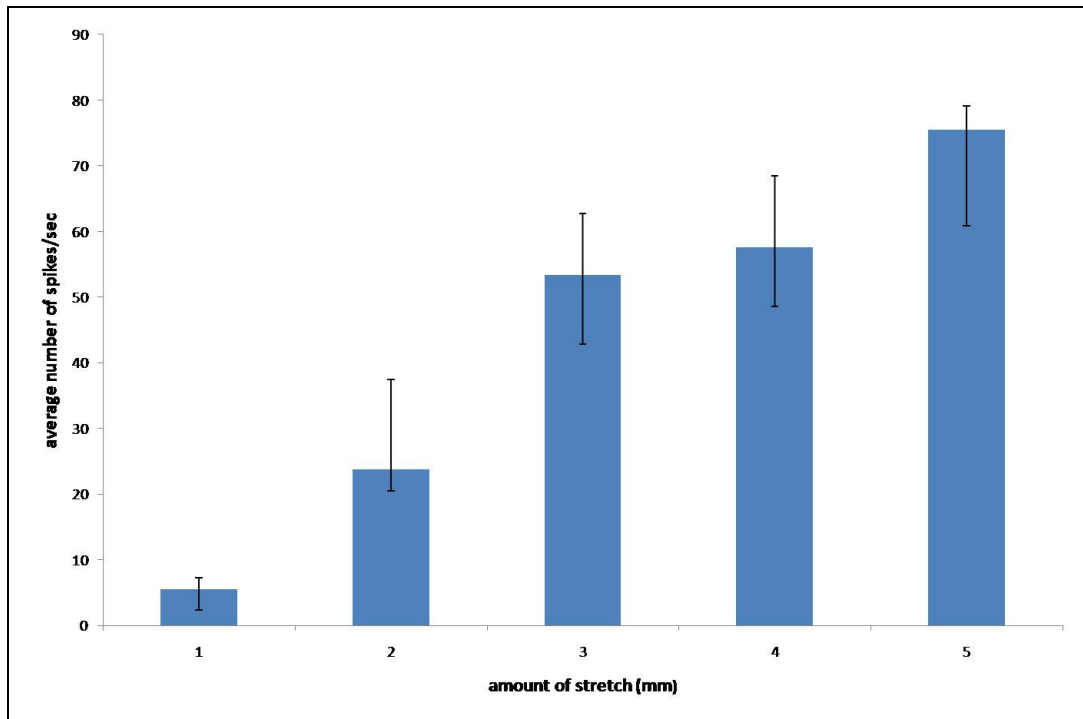


Figure 3.4 Relationship between amount of gastrocnemius stretch and firing rate for gastrocnemius muscle.

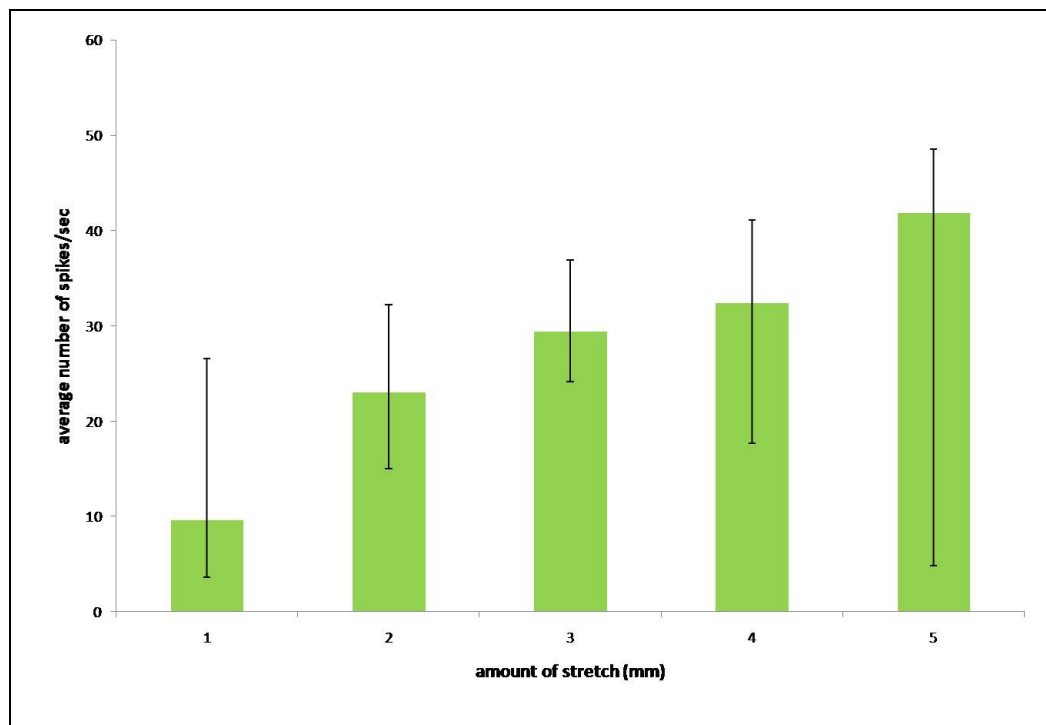


Figure 3.5 Relationship between amount of gastrocnemius stretch and firing rate for lengthwise restrained antagonist muscle.

loading gastrocnemius with displacement yield afferent response in both gastrocnemius and antagonist afferents and different stretch amplitudes. For stretches over 2 mm, firing rates of gastrocnemius afferents are higher than antagonist afferents, suggesting load is only partially transmitted via epimuscular pathways, however high variance of antagonist data makes it difficult to conclude for 1 and 2 mm of stretch.

4. DISCUSSION

4.1 Effects of Passive Stretch

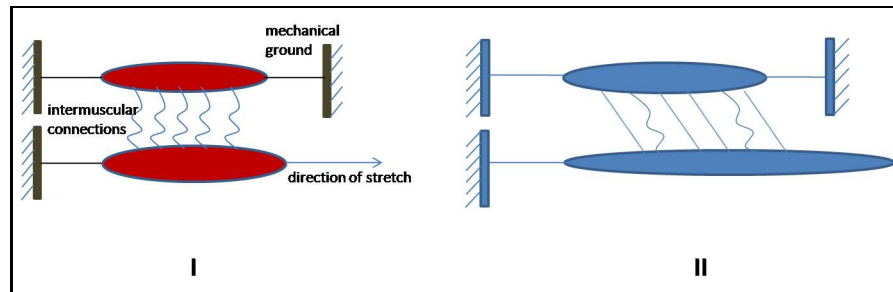


Figure 4.1 Intermuscular connections transmit force on gastrocnemius muscle caused by stretch.

Stretching gastrocnemius puts tensile force on it and shear forces dominate in the antagonist through the intermuscular connections (see Figure 4.1). Increasing the stretch amplitude results in increased tensile load on the responding fiber, thus the firing rates reach to higher values. The assumption, which the hypothesis is of this work is built on, that passive stretch on gastrocnemius muscle will cause a stress distribution on the antagonist muscle group has been supported by modeling studies [13]. In a series of experiments in rat and supporting modeling studies, where EDL muscle of the lower leg was lengthened and its synergists TA+EHL complex remained at constant length, it was revealed that in addition to alterations in force generation of both muscle groups, there is varying stress on different parts of the muscles. Length change in EDL caused the stress on lengthwise restrained TA+EHL complex to vary. Similarly stretch of gastrocnemius is expected to change the stress distributions on antagonist group and therefore individual fibers of the antagonist group would be strained differently. On the other hand the antagonist group muscles don't change length therefore strain caused by the transmitted force on one part of the muscle must be countered on the other part in order to overall fiber length be constant.

4.2 Changes in Response with Different Stretch Amplitude

The result showing that with increasing stretch amplitude the firing rate increases is more prominent in directly stretched gastrocnemius than the restrained antagonist. In the latter group the variance is too big to tell the quality of the correlation. The Figures 4.2 and 4.3 shows the behavior of the sensory fibers at each individual experiment.

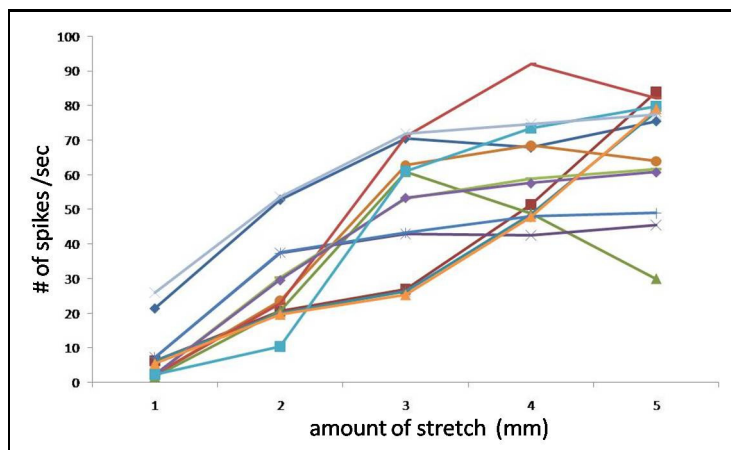


Figure 4.2 Spike rate at different lengths for individual gastrocnemius afferent units.

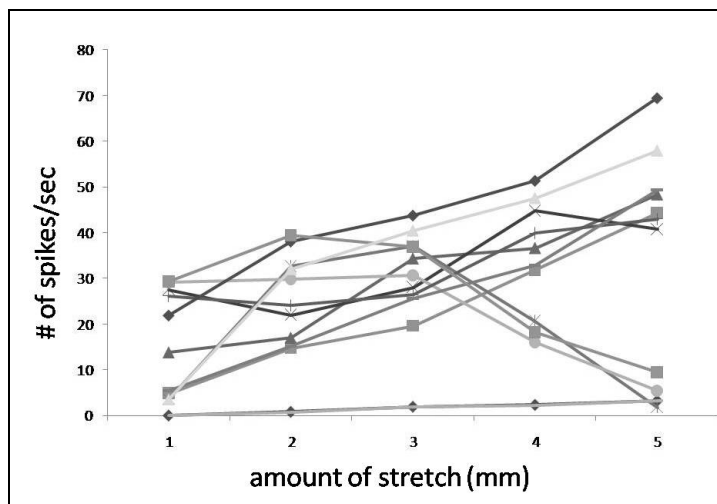


Figure 4.3 Spike rate at different lengths for individual antagonist afferent units.

It can be noticed that overall units increase firing when the stretch amplitude is increased. However some outliers are also noticeable. These outliers are more distinct in antagonist group. Varying strain distributions throughout the muscle imposes heterogeneity in individual sarcomere lengths [16]. In other words in a muscle fiber

comprised of series of sarcomeres, the length of individual sarcomeres might vary due to local strain distributions. If due to such distributions, an intrafusal fiber, on which the capsule of a muscle spindle resides, endures less stress than its neighbor, it is conceivable that its firing will not increase even if the overall muscle length increases.

This notion also explains the individual outliers in the recordings. In Figure 4.3 there is an individual unit that increases firing with stretch and then drops after 3 mm and there is also one that starts with a certain rate and then drops off. Changes in local stress distributions of those units might have caused such effects. Joint angles can also be a key determinant in that response. Since muscle operate at different lengths at different joint angles, starting with a different selection of hip-knee-ankle angles other than the ones used in this work might result in different firing characteristics.

4.3 Limitations of the Study

It might be argued against that unit spikes are sorted on amplitude basis only. Recorded spike amplitude is dependant on two parameters: The diameter of the nerve being recorded from and the distance of the electrode tip to the nerve [29]. The electrode was fairly stable throughout the experiments, yet information on diameters of the recorded nerves was not available.

Myofascial force transmission has also been shown to occur between antagonists [30]. However this has not been demonstrated for frogs. In addition to that, there are some important anatomical differences between frogs and rats. For example the interosseal membrane, which is regarded as an important structure in extramuscular force transmission, is not present in frogs. In frog skeletal system the lower leg has a single bone called tibia-fibula that separates the antagonist muscle groups. However, it has been demonstrated that lateral force transmission occurs in frog myofibers [31] and the epimysia of these muscles are also continuous and so is the neurovascular tract therefore the idea that intermuscular and extramuscular force transmission occurs in frog lower leg is conceivable.

The point can be raised if this work offers any better method to investigate the effects of myofascial force transmission than direct force measurements. When the afferent signals traced to the individual fiber they originate in, these recordings might be used as an indirect measurement for the percentage of myofascial effects in the musculoskeletal system when direct force measurement is only possible by disintegration of the system. The results show that for a given amount of stretch the response in directly stretched muscle is higher than the antagonists owing to force being partially transmitted. There are several investigations on how to relate the intensity of the stimulus to the afferent response, e.g. [32]. A method is the Fechner's rule that foresee geometric increase in the stimulus amplitude to match an arithmetic increase in response ($S=a*\log R+b$) where S is stimulus intensity, R is the response and a and b are constants [33]. In a more precisely controlled system, by using the drop in firing rate as the known variable of the above equation, it might be possible to calculate the percentage of the force transmitted via epimuscular ways.

APPENDIX A. MATLAB CODE FOR SINGLE UNIT SPIKE SORTING

```

function [raw] = ikiknl(file)

[raw, Fs] = wavread(strcat(file, '.wav'));
disc = raw(:,2);
undisc = raw(:,1);
t = [linspace(0,length(raw)/Fs,length(raw))]';

%smooth the ridges
y = zeros(length(undisc),1);
L = 4;
L1 = L+1;
L2 = 2*L+1;
y(L+1)= sum(undisc(1:L2));

for i=(L+2):(length(undisc)-L)
    y(i)=sum( undisc((i-L):(i+L)) );
end

y=y/L2;
%smooth the ridge end

d = zeros(length(y),1);
u = zeros(length(y),1);

spikes=zeros(length(y),1);
NumberOfPeaks=0;
eventtime=zeros(NumberOfPeaks,1);

```

```

plot(y((Fs*11):(Fs*12)))

>window aperture
thr=ginput;
close all

for i=1:1:length(y);
    d(i)=max(thr(:,2));
    u(i)=min(thr(:,2));
    if y(i)<d(i) && y(i)>u(i) && y(i)<y(i-1) && y(i)<y(i+1)
        spikes(i)=1;
        NumberOfPeaks = NumberOfPeaks+1;
        eventtime(NumberOfPeaks,1) = i;
    end
end
>window aperture defined

%take out non-events
counts=0;
et = zeros(counts,1);
non_event=((Fs/1000)*2);

for i=2:1:length(eventtime)
    if eventtime(i)-eventtime(i-1) > non_event;
        counts=counts+1;
        et(counts,1)=eventtime(i);
    end
end
et=[eventtime(1); et];
%non_events taken out

```

```
save(strcat(file, '.mat'), 'Fs', 'undisc', 't', 'y', 'thr', 'counts',  
'et', 'spikes', 'eventtime', 'NumberOfPeaks', 'pre', 'peri', 'post')
```

REFERENCES

1. Guyton, A. J., and J. E. Hall, *Textbook of Medical Physiology*, 11th ed., Chapter 6, Philadelphia: Elsevier Saunders, 2006.
2. Neumann, D. A., *Kinesiology of the Musculoskeletal System*, Section 1, St. Louis: Mosby, 2002.
3. MacIntosh, B. R., P. F. Gardiner, and A. J. McComas, *Skeletal Muscle: Form and Function*, 2nd ed., Chapter 4, Human Kinetics, 2006.
4. Alberts, B., A. Johnson, J. Lewis, M. Raff, K. Roberts, and P. Walter, *Molecular Biology of the Cell*, 4th ed., New York: Garland Science, 2002.
5. Huxley, H., and J. Hanson, "Changes in the cross striations of muscle during contraction and stretch and their structural interpretation," *Nature*, Vol. 173, pp. 973–976, 1954.
6. Huxley, A., and J. Hanson, "Structural changes in muscle during contraction, interference microscopy of living muscle fibers," *Nature*, Vol. 173, pp. 971–973, 1954.
7. Huijing, P. A., "Muscle as a collagen fiber reinforced composite: a review of force transmission in muscle and whole limb," *Journal of Biomechanics*, Vol. 32, pp. 329–345, 1999.
8. Loeb, G. E., C. A. Pratt, C. M. Chanaud, and F. J. Richmond, "Distribution and innervation of short, interdigitated muscle fibers in parallel fibered muscles of the cat hindlimb," *Journal of Morphology*, Vol. 191, pp. 1–15, 1987.
9. Huijing, P. A., "Muscular force transmission: A unified, dual or multiple system? A review and some explorative experimental results," *Archives of Physiology and Biochemistry*, Vol. 170, pp. 292–311, 1999.
10. Street, S. F., "Lateral transmission of tension in frog myofibers: a myofibrillar network and transverse cytoskeletal connections are possible transmitters," *Journal of Cellular Physiology*, Vol. 114, pp. 146–364, 1983.
11. Trotter, J. A., and P. P. Purslow, "Functional morphology of the endomysium in series fibered muscles," *Journal of Morphology*, Vol. 212, pp. 109–122, 1992.
12. Huijing, P. A., G. C. Baan, and G. Rebel, "Non myo-tendinous force transmission in rat extensor digitorum longus," *Journal of Experimental biology*, Vol. 201, pp. 682–691, 1998.

13. Yücesoy, C. A., B. H. F. J. M. Koopman, G. C. Baan, H. J. Grootenboer, and P. A. Huijing, "Effects of inter and extramuscular myofascial force transmission on adjacent synergistic muscles: assessment by experiments and finite element modeling," *Journal of Biomechanics*, Vol. 36, pp. 1797–1811, 2003.
14. Maas, H., G. C. Baan, and P. A. Huijing, "Intermuscular interaction via myofascial force transmission: effects of tibialis anterior and extensor hallucis longus length on force transmission from rat extensor digitorum longus muscle," *Journal of Biomechanics*, Vol. 34, pp. 927–940, 2001.
15. Yücesoy, C. A., H. J. F. M. Koopman, G. C. Baan, H. J. Grootenboer, and P. A. Huijing, "Extramuscular myofascial force transmission: Experiments and finite element modeling," *Archives of Physiology and Biochemistry*, Vol. 111, pp. 377–388, 2003.
16. Yücesoy, C. A., *Intra-, inter- and extra-muscular myofascial force transmission: A combined finite element modeling and experimental approach*. PhD thesis, University of Twente, Utrecht, The Netherlands, 2003.
17. Maas, H., G. C. Baan, P. A. Huijing, C. A. Yücesoy, B. H. J. F. M. Koopman, and H. J. Grootenboer, "The relative position of edl muscle affects the length of sarcomeres within muscle fibers: experimental results and finite element modeling," *Journal of Biomechanical Engineering*, Vol. 125, pp. 745–753, 2003.
18. Llinas, R., and W. Precht, eds., *Frog Neurobiology, a handbook*, Chapter 22, Heidelberg: Springer-Verlaag, 1976.
19. Matthews, P. B. C., "Muscle spindles and their motor control," *Physiological Reviews*, Vol. 44, pp. 219–288, April 1964.
20. Brokensha, G., and D. R. Westbury, "Adaptation of the discharge of frog muscle spindles following a stretch," *Journal of Physiology*, Vol. 242, pp. 383–403, 1974.
21. Gizster, S. F., and W. J. Kargo, "Seperation and estimation of muscle spindle and tension receptor populations by vibration of the biceps muscle in the frog," *Archives Italiennes de Biologie*, Vol. 140, pp. 283–294, 2002.
22. Dunn, E. H., "On the number and on the relation between diameter and distribution of the nerve fibers innervating the leg of the frog," *Journal of Comperative Neurology*, Vol. 10, no. 2, pp. 218–242, 1900.

23. Güçlü, B., "Low cost computer controlled current stimulator for the student laboratory," *Advanced Physiological Education*, Vol. 31, pp. 223–231, 2007.
24. Mutlu, S., "The effects of serotonin and its antagonists on slowly adapting type I mechanoreceptive fibers in frog skin," Master's thesis, Bogazici University, Istanbul, Turkey, 2008.
25. Uçar, K., "Classification of tactile units of frogs by using von frey monofilaments," Master's thesis, Bogazici University, Istanbul, Turkey, 2006.
26. Matthews, B. H. C., "The response of a single end organ," *Journal of Physiology*, Vol. 61, pp. 64–110, 1931.
27. Stuart, D. G., G. E. Goslow, C. G. Mosher, and R. M. Reinking, "Stretch responsiveness of golgi tendon organs," *Experimental Brain Research*, Vol. 10, no. 5, pp. 463–476, 1970.
28. De-Doncker, L., F. Picquet, J. Petit, and M. Falempin, "Characterization of spindle afferents in rat soleus muscle using ramp-and-hold and sinusoidal stretches," *Journal of Neurophysiology*, Vol. 89, pp. 442–449, 2003.
29. Hunt, C. C., "Relation of function to diameter in afferent fibers of muscle nerves," *Journal of General Physiology*, Vol. 38, pp. 117–131, 1954.
30. Rijkelijhuizen, J. M., H. J. M. Meijer, G. C. Baan, and P. A. Huijing, "Myofascial force transmission also occurs between antagonistic muscles located within opposite compartments of the rat lower hind limb," *Journal of Electromyography and Kinesiology*, Vol. 17, pp. 690–697, 2007.
31. Ramsey, R. W., and S. F. Street, "The isometric length-tension diagram of isolated skeletal muscle fibers of the frog," *Journal of Cellular and Comparative Physiology*, Vol. 15, pp. 11–34, 1940.
32. Eckhorn, R., and H. Querfurth, "Information transmission by isolated frog muscle spindle," *Biological Cybernetics*, Vol. 52, pp. 165–176, 1985.
33. Granit, R., *Receptors and Sensory Perception*, New Haven: Yale University Press, 1955.